Two dimensional coordination polymers based on 3,5-di(1H-imidazol-1-yl)pyridine and their fluorescence properties

Hao Zhang,[a,§] Zhao Qiang Zhu,[a,§] Fu-Hou Zhou,[a] Carl Redshaw,[c] Kai Chen[a,*], Jing Xu [a, b]*

[a] School of Chemistry and Materials Science, Nanjing University of Information Science & Technology, Jiangsu, Nanjing, 210044, *P. R. China. Email: xujing2003246@163.com* (J. Xu).

[a] *Collaborative Innovation Center of Atmospheric Environment and Equipment Technology, Jiangsu Key Laboratory of Atmospheric Environment Monitoring and Pollution Control, School of Environmental Science and Engineering, Nanjing University of Information Science & Technology, Nanjing 210044, P. R. China. Email: catgchen@163.com or kaichen85@nuist.edu.cn*

[c] *Department of Chemistry, University of Hull, Hull HU6 7RX, UK.*

[§] H. Zhang and Z.-Q. Zhu contributed equally to this work. The authors declare no competing financial interest.

Abstract: The solvothermal synthesis of three new 2D MOFs is reported. Reaction of 3,5-di(1H-imidazol-1-yl)pyridine (dip), and the metal salts $Co(NO_3)_2 \cdot 6H_2O$, $Cd(NO_3)_2 \cdot 4H_2O$ and $Zn(NO_3)_2 \cdot 4H_2O$, the three MOFs $[Co(dip)_2(SCN)_2]$ (**1**), $\{[Cd(dip)_2(H_2O)_2] \cdot (NO_3)_2\}$ (**2**), $\{[Zn(dip)_2(H_2O)_2] \cdot (ClO_4)_2\}$ (**3**) were obtained. For these 2D MOFs, all the metal ions adopted six-coordinated octahedral geometry with axial coordination sites occupied by SCN^- or water molecules. They were all monocoordinated and thus render the linkage of layered MOFs structure. Furthermore, the fluorescence properties of **2** and **3** have been investigated.

Introduction

Metal-organic frameworks (MOFs) are crystalline materials synthesized by the self-assembly of organic ligands and metal ions or clusters.[1] In the past several decades, they have attracted considerable attention due to their tailorable structure, porous character and large surface area. They have been investigated as potential functional materials in different areas, such as gas storage, catalysis, energy storage, luminescent materials, and solar energy utilization and so on.[2-14] Among all the reported coordination polymers, three-dimensional (3D) coordination polymers have received most focus given their rigid frameworks and available porosity, while two-dimensional (2D) coordination polymers have received comparatively little attention. Since the discovery of graphene, 2D nanomaterials have become immensely intriguing to researchers all over the world.[15-17] With the rapid development of 2D nanomaterials, 2D MOF nanosheets have emerged as a topical area and have been investigated as platforms for different applications.[18-25] Because the common methods to prepare 2D MOF nanosheets involve the exfoliation of bulk layer-structured MOFs, the synthesis of 2D MOFs have also received increasing research interest.[7, 23]

 In typical syntheses of 2D MOFs, the central metal ions or clusters usually adopt a planar coordination geometry or 3D polyhedral coordination geometry with the axial coordination sites occupied by mono-coordinated species.[26] For example, Bao and co-workers reported the first synthesis of a new 2D conductive MOFs using the oxygen analog of $Cu_3(C_6X_6)_2$ (X = NH, S, O) family, which was obtained on the basis of the planar quadrilateral coordination geometry of the

central metal ions.[27] Kitagawa and coworker reported the synthesis of CoTCPP-py-Cu nanosheets using the interfacial synthesis method and in these nanosheets, pyridine was introduced as the auxiliary ligand and occupied the axial coordination sites of the Cu-based paddle-wheel substructure, which thus restrain the linkage of the layered coordination structure.[28]

Based on the strategy employing mono-coordinated species to prevent the further extension of 2D coordination structure, we here report the synthesis of three novel 2D MOFs by the reaction of 3,5-di(1H-imidazol-1-yl)pyridine (dip) with the transition metal salts $Co(NO_3)_2 \cdot 6H_2O$, $Cd(NO_3)_2 \cdot 4H_2O$ and $Zn(NO_3)_2 \cdot 4H_2O$ under solvothermal conditions. Products with the formulae $[Co(dip)_2(SCN)_2]$ (**1**), $\{[Cd(dip)_2(H_2O)_2] \cdot (NO_3)_2\}$ (**2**), $\{[Zn(dip)_2(H_2O)_2] \cdot (ClO_4)_2\}$ (**3**) were isolated. In these three 2D MOFs, all the metal ions possess an octahedral geometry and four nitrogen atoms from the imidazole units, which are located in the coordination plane, while the anion SCN^- or water molecules bind to metal ions in the axial direction in mono-coordinated mode, which thus results in the 2D coordination structure. The final 3D supramolecular frameworks are generated through various non-covalent interactions, such as $\pi \cdots \pi$ and C-H$\cdots\pi$ interactions. Furthermore, the fluorescence properties of **2** and **3** have been investigated.

Experimental Section

Materials and methods

The organic compound dip was synthesized following a previously published procedure.[29] All other commercially available chemicals and solvents are of reagent grade and were used without further purification. Elemental analyses for C, H and N were performed on a Perkin-Elmer 240C Elemental Analyzer at the analysis center of Nanjing University. FT-IR spectra were recorded in the range of 400 - 4000 cm^{-1} on a Bruker Vector22 FT-IR spectrophotometer using KBr pellets. Powder X-ray diffraction (PXRD) measurements were carried out on a Bruker D8 Advance X-ray diffractometer using Cu-Kα radiation (λ = 1.5418 Å), in which the X-ray tube was operated at 40 kV and 40 mA. Thermal gravimetric analyses (TGA) were taken on a Mettler-Toledo (TGA/DSC1) thermal analyzer under an N_2 atmosphere with a heating rate of 10 ℃ min^{-1}. The fluorescence spectra were measured on a Perkin Elmer LS-55 fluorescence spectrophotometer.

Synthesis of **[Co(dip)$_2$(SCN)$_2$] (1)**. A mixture of dip (6.33 mg, 0.03 mmol), $Co(NO_3)_2 \cdot 6H_2O$ (26.2 mg, 0.09 mmol), *N,N*-dimethylformamide (DMF) (4 mL) and H_2O (4 mL) was sealed in Teflon-lined stainless steel container and heated at 90 ℃ for 3000 min. After being cooled to room temperature, yellow block crystals of **1** were obtained in 47% yield. Anal. Calcd for $C_{24}H_{18}CoN_{12}S_2$: C 48.24, H 3.03, N 28.13 %. Found: C 48.22, H 3.08, N 28.19 %. IR (KBr pellet, cm^{-1}): 3458 (m), 2913 (w), 2560 (w), 1938 (m), 1622 (m), 1487 (s), 1335 (w), 1305 (w), 1295 (w), 1288 (w), 1258 (s), 1082 (s), 923 (w), 898 (w), 822 (m), 770 (w), 698 (w), 627 (m).

Synthesis of **{[Cd(dip)$_2$(H$_2$O)$_2$]·(NO$_3$)$_2$} (2)**. A mixture of dip (6.33 mg, 0.03 mmol), $Cd(NO_3)_2 \cdot 4H_2O$ (27.76 mg, 0.03 mmol), *N,N*-dimethylformamide (DMF) (3 mL) and H_2O (7 mL) was sealed in Teflon-lined stainless steel container and heated at 90 ℃ for 3000 min. After being cooled to room temperature, yellow block crystals of **2** were obtained in 41% yield. Anal. Calcd for $C_{22}H_{22}CdN_{12}O_8$: C 38.02, H 3.19, N 24.18 %. Found: C 38.08, H 3.14, N 24.22%. IR (KBr pellet, cm^{-1}): 3395 (m), 1605 (m), 1514(s), 1452 (w), 1396(s), 1358 (s), 1322 (s), 1250 (m), 1125 (w), 1072 (m), 1067 (m), 992 (w),863 (w), 853 (w), 765 (w), 735 (m), 688 (m), 669 (m).

Synthesis of **{[Zn(dip)$_2$(H$_2$O)$_2$]·ClO$_4$)$_2$} (3)**. A mixture of dip (6.33 mg, 0.03 mmol), $Zn(NO_3)_2 \cdot 4H_2O$ (26.73 mg, 0.09 mmol), $NaClO_4$ (12.64 mg, 0.09 mmol), *N,N*-dimethylformamide (DMF, 3 mL) and H_2O (7 mL) was sealed in Teflon-lined stainless steel

container and heated at 85 ℃ for 3000 min. After being cooled to room temperature, yellow block crystals of **1** were obtained in 47% yield. Anal. Calcd for $C_{22}H_{22}Cl_2N_{10}O_{10}Zn$: C 38.02, H 3.19, N 24.18 %. Found: C 38.08, H 3.14, N 24.22%. IR (KBr pellet, cm^{-1}): 3409 (w), 1610 (m), 1608 (m),1521 (s), 1466 (w), 1329 (w), 1268 (m), 1085 (s), 956 (m), 892 (m), 829 (m), 731 (m), 695 (m), 642 (m), 627 (s), 617 (s).

X-Ray crystallography

The crystallographic data collections for **1** - **3** were carried out on a Bruker Smart Apex II CCD area-detector diffractometer with graphite-monochromated Mo Kα radiation (λ = 0.71073 Å) at 293(2) K using ω-scan technique. The diffraction data were integrated by using the *SAINT* program,[30] which was also used for the intensity corrections for the Lorentz and polarization effects. Semi-empirical absorption correction was applied using the *SADABS* program.[31] The structures were solved by direct methods and all the non-hydrogen atoms were refined anisotropically on F^2 by the full-matrix least-squares technique using the SHELXL-97 crystallographic software package.[32] All non-hydrogen atoms were refined anisotropically. Hydrogen atoms of the water molecules were located from the difference Fourier maps and refined with restraint of the O-H and H···H distance (0.96 Å and 1.52 Å, respectively). Other hydrogen atoms were introduced at the calculated positions. The details of the crystal parameters, data collection and refinements for the complexes are summarized in **Table 1**, and selected bond lengths and angles with their estimated standard deviations are listed in **Table 2**.

Table 1. Crystal Data and Structure Refinements for **1** - **3**.

Compounds	1	2	3
Formula	$C_{24}H_{18}CoN_{12}S_2$	$C_{22}H_{22}CdN_{12}O_8$	$C_{22}H_{22}Cl_2N_{10}O_{10}Zn$
Formula weight	597.55	694.92	722.79
T (K)	273(2)	291(2)	293(2)
Crystal system	Monoclinic	Monoclinic	Monoclinic
Space group	$P2_1/c$	$P2_1/n$	$P2_1/n$
a (Å)	17.234(3)	9.5144(9)	8.7651(1)
b (Å)	9.2012(14)	10.5036(10)	10.4828(12)
c (Å)	16.812(3)	13.8018(13)	15.0674(18)
β (°)	106.007(3)	104.512(2)	96.937(2)
V (Å^3)	2562.5(7)	1335.3(2)	1374.3(3)
Z	4	2	2
D_{calc} (g cm^{-3})	1.549	1.728	1.747
μ (mm^{-1})	0.874	0.890	1.165
$F(000)$	1220	700	736
Reflections collected	10557	6978	6609
Unique reflections	4291	2614	2408
Goodness-of-fit on F^2	1.180	1.115	1.104
R_1,	0.1069	0.0445	0.0399
wR_2 [I > 2σ(I)]^{a,b}	0.2587	0.1180	0.1148
R_1,	0.1272	0.0482	0.0418

wR_2 [all data]	0.2724	0.1206	0.1167

$^aR_1 = \Sigma||F_o| - |F_c||/\Sigma|F_o|.$ $^bwR_2 = |\Sigma w(|F_o|^2 - |F_c|^2)|/\Sigma|w(F_o)^2|^{1/2}$, where $w = $ m$= 1/[\sigma^2(F_o^2) +(aP)^2+bP]$. P = $(F_o^2 + 2F_c^2)/3$

Table S1. Selected bond lengths (Å) and angles (°) for assembly **1 – 3**.

1			
Co(1)-N(1)	2.120(6)	Co(1)-N(12)#1	2.131(6)
Co(1)-N(7)	2.139(6)	Co(1)-N(6)	2.141(6)
Co(1)-N(8)	2.152(6)	Co(1)-N(5)#2	2.153(6)
N(1)-Co(1)-N(12)#1	179.7(2)	N(1)-Co(1)-N(7)	89.9(2)
N(12)#1-Co(1)-N(7)	90.4(2)	N(1)-Co(1)-N(6)	90.9(2)
N(12)#1-Co(1)-N(6)	88.8(2)	N(7)-Co(1)-N(6)	178.6(2)
N(1)-Co(1)-N(8)	89.5(2)	N(12)#1-Co(1)-N(8)	90.5(2)
N(7)-Co(1)-N(8)	92.6(2)	N(6)-Co(1)-N(8)	88.5(2)
N(1)-Co(1)-N(5)#2	91.8(2)	N(12)#1-Co(1)-N(5)#2	88.2(2)
N(7)-Co(1)-N(5)#2	88.2(2)	N(6)-Co(1)-N(5)#2	90.7(2)
N(8)-Co(1)-N(5)#2	178.5(2)		
2			
Cd(1)-O(1)	2.312(3)	Cd(1)-N(3)#3	2.317(3)
Cd(1)-N(5)	2.344(3)		
O(1)-Cd(1)-O(1)#2	180.0	O(1)-Cd(1)-N(3)#3	88.00(12)
O(1)#2-Cd(1)-N(3)#3	92.00(12)	N(3)#3-Cd(1)-N(3)#4	180.0
O(1)-Cd(1)-N(5)	83.90(12)	O(1)#2-Cd(1)-N(5)	96.10(12)
N(3)#3-Cd(1)-N(5)	92.36(12)	N(3)#4-Cd(1)-N(5)	87.64(12)
N(5)-Cd(1)-N(5)#2	180.0		
3			
Zn(1)-O(1)	2.1166(16)	Zn(1)-N(5)	2.1431(19)
Zn(1)-N(1)#2	2.1823(19)		
O(1)-Zn(1)-O(1)#1	180.00(10)	O(1)-Zn(1)-N(5)#1	88.43(7)
O(1)#1-Zn(1)-N(5)#1	91.57(7)	O(1)-Zn(1)-N(5)	91.57(7)
O(1)#1-Zn(1)-N(5)	88.43(7)	N(5)#1-Zn(1)-N(5)	180.00(14)
O(1)-Zn(1)-N(1)#2	87.42(7)	O(1)#1-Zn(1)-N(1)#2	92.58(7)
N(5)#1-Zn(1)-N(1)#2	91.95(7)	N(5)-Zn(1)-N(1)#2	88.05(7)
O(1)-Zn(1)-N(1)#3	92.58(7)	O(1)#1-Zn(1)-N(1)#3	87.42(7)
N(5)#1-Zn(1)-N(1)#3	88.05(7)	N(5)-Zn(1)-N(1)#3	91.95(7)
N(1)#2-Zn(1)-N(1)#3	180.00(10)		

Symmetry transformations used to generate equivalent atoms: #1 x,-y+5/2,z+1/2, #2 x,-y+3/2,z+1/2, #3 x,-y+3/2,z-1/2, #4 x,-y+5/2,z-1/2 for **1**; #1 -x-1/2,y-1/2,-z+1/2, #2 -x,-y+2,-z, #3 x+1/2,-y+3/2,z-1/2, #4 -x-1/2,y+1/2,-z+1/2 for **2**; #1 -x+2,-y,-z, #2 -x+3/2,y-1/2,-z+1/2, #3 x+1/2,-y+1/2,z-1/2, #4 -x+3/2,y+1/2,-z+1/2 for **3**.

Results and discussion

Crystal structure descriptions

Crystal Structure of [Co(dip)$_2$(SCN)$_2$] (1). X-ray single-crystal diffraction analysis reveals that **1** crystallizes in the monoclinic crystal system with space group of $P2_1/c$. The asymmetric unit

contains one Co(II) ion, two ligands dip and two SCN$^-$ anions. As shown in Figure 1a, each Co atom is located in an octahedral coordination geometry surrounded by six nitrogen atoms, in which four nitrogen atoms (N1, N5#2, N8, N12#1) are from four different dip ligands and the other (N6, N7) two are from the coordinated SCN$^-$ anions. The Co-N bond lengths are in the range 2.120(6) - 2.153(6) Å and N-Co-N bond angles are in the range 88.2(2) - 179.7(2)° (Table S1). Further inspection reveals that the four coordinated nitrogen atoms from ligands around one central metal ion are coplanar and each dip coordinates with two Co(II) cations, which results in the formation of 2D coordination bilayers (Figure 1b). The mono-coordinated SCN$^-$ anions are bound to Co(II) cations in the axial directions, which prevent further extension of these 2D layers. These layers interact with each other to generate the final 3D supramolecular frameworks (Figure 1c) through C-H⋯π interactions (3.031 and 3.215 Å, Figure 1d).
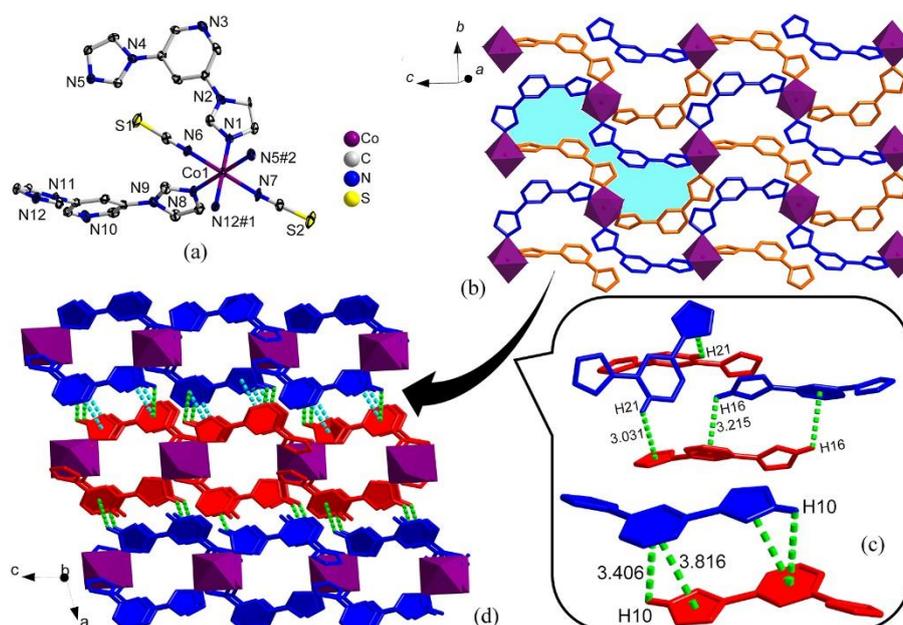
Figure 1. (a) Coordination environment of Co(II) in **1** with the ellipsoids drawn at the 30% probability level. The hydrogen atoms are omitted for clarity. (b) Top view of the 2D coordination structure in **1**. (c) The interactions between ligands dip from different layers. (d) The final 3D supramolecular framework of **1**.

Crystal Structure of {[Cd(dip)$_2$(H$_2$O)$_2$]·(NO$_3$)$_2$} (2). When the metal salt employed was Cd(NO$_3$)$_2$, complex **2** could be obtained. SC-XRD analysis reveals that compound **2** crystallized in the monoclinic crystal system with space group of $P2_1/n$ and each asymmetric unit in **2** consists of one half Cd(II) cation, one dip ligand, one coordinated water molecule and one free NO$_3^-$ anion. As shown in Figure 2a, each Cd atoms adopted an octahedral geometry and is coordinated by four nitrogen atoms (N3#3, N3#4, N5, N5#2) from four adjacent dip and two oxygen atoms (O1, O1#2) from coordinated water molecules. The binding of Cd(II) ions to the organic ligand dip generates the 2D bilayer coordination structure. The presence of the mono-coordinated water molecules in the axial directions prevents the formation of 3D coordination networks. The final 3D supramolecular structure is constructed through π⋯π and C-H⋯π interactions between the layers. Furthermore, there is a hole in the octahedron constructed by six adjacent Cd(II) ions and each hole can accommodate two NO$_3^-$ anions.
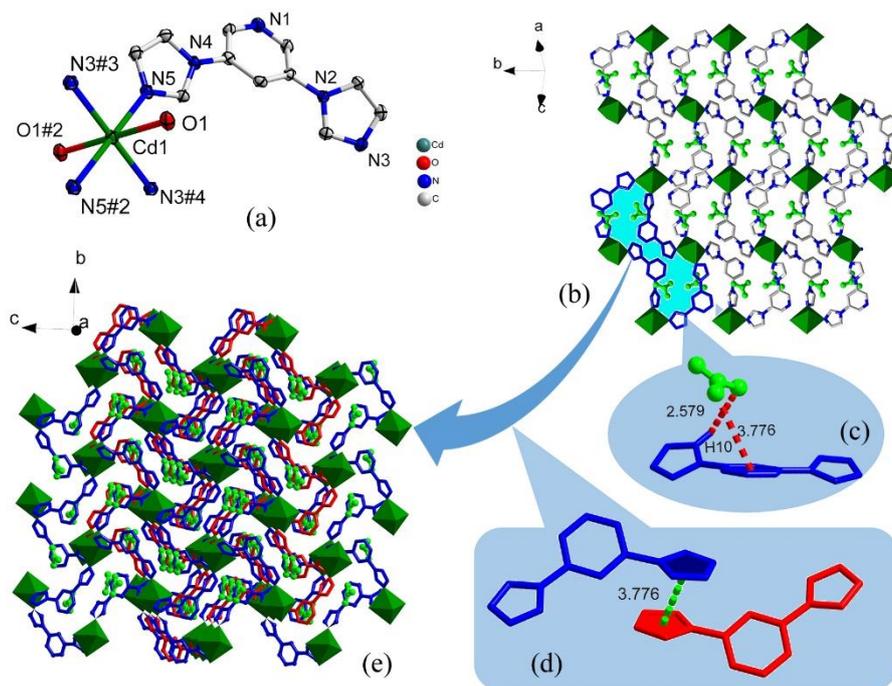
Figure 2. (a) Coordination environment of Cd(II) in **2** with the ellipsoids drawn at the 30% probability level. The hydrogen atoms are omitted for clarity. (b) Top view and side view of the 2D coordination structure in **2**. (c) The interaction between the NO_3^- anion and ligand dip. (d) The interactions between ligands dip from different layers. (e) The final 3D supramolecular framework of **2**.

Crystal Structure of {[Zn(dip)$_2$(H$_2$O)$_2$]·(ClO$_4$)$_2$} (3). According to the SC-XRD analysis, compound **3** also crystallized in the monoclinic crystal system with space group of $P2_1/n$ and its asymmetric unit contains one half Zn(II) cation, one dip molecule, one coordinated water molecule and one free ClO_4^- anion. As for **2**, the Zn atom in compound **3** is also coordinated by four nitrogen atoms (N1#2, N1#3, N5, N5#1) from four adjacent dip ligands and two oxygen atoms (O1, O1#2) from coordinated water molecules in an octahedral coordination geometry. In the coordination octahedron, four nitrogen atoms are located in the plane and the water molecules bind to the central Zn atom in axial directions, which thus resulted in the 2D bilayered coordination structure. Moreover, the final supramolecular 3D framework could be generated through π···π and C-H···π interactions. Furthermore, similar to **2**, each six adjacent Zn(II) cations from different bilayers form an octahedral supramolecular cage, which accommodates two ClO_4^- anions.
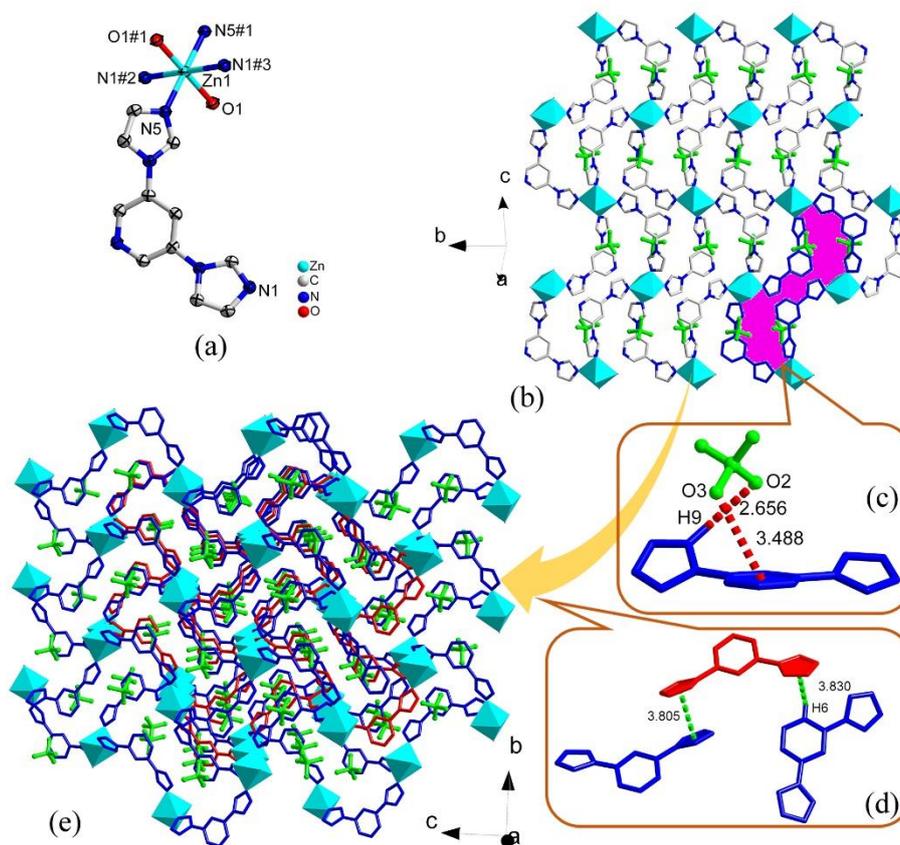
Figure 3. (a) Coordination environment of Zn(II) in **3** with the ellipsoids drawn at the 30% probability level. The hydrogen atoms are omitted for clarity. (b) Top view and side view of the 2D coordination structure in **3**. (c) The interaction between the ClO_4^- anion and ligand dip. (d) The interactions between ligands dip from different layers. (e) The final 3D supramolecular framework of **3** and The interactions between ligands dip from different layers.

PXRD and Thermostability studies

PXRD was employed to check the phase purity. As depicted in Figure 4, all the peaks displayed in the experimental patterns were consistent with the simulated patterns obtained according to the single-crystal diffraction data, which confirmed the phase purity.
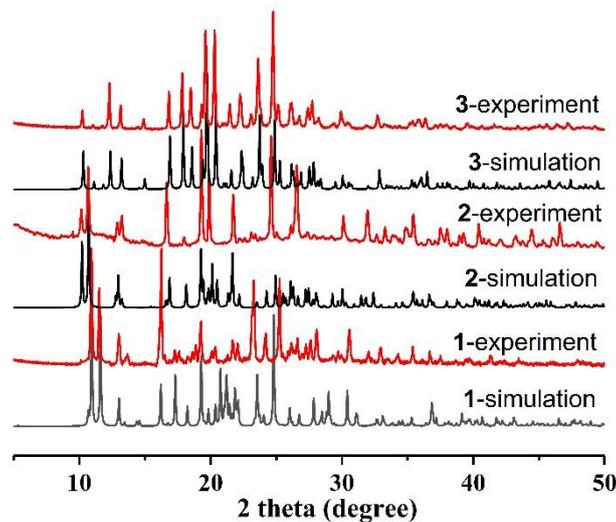
Figure 4. PXRD patterns for **1**-**3** under ambient conditions: simulated (black) and as-synthesized (red).

TGA was conducted to investigate the thermal stability of **1** - **3**. As shown in **Figure 5**, the TG curve of **1** displayed no obvious weight loss before 300 °C, which is in accordance with the fact that there are no guest molecules present. The framework of compound **1** then began to collapse after 300 °C. According to the TGA results, compounds **2** and **3** exhibited similar characteristics, and showed no obvious weight loss before 150 °C followed by a weight loss of 5.22 and 4.93% in 150 - 200 °C assigned to the release of coordinated water molecules (calcd. 5.19 and 4.98 %), respectively. Their frameworks are stable up to 350 and 380 °C, respectively.
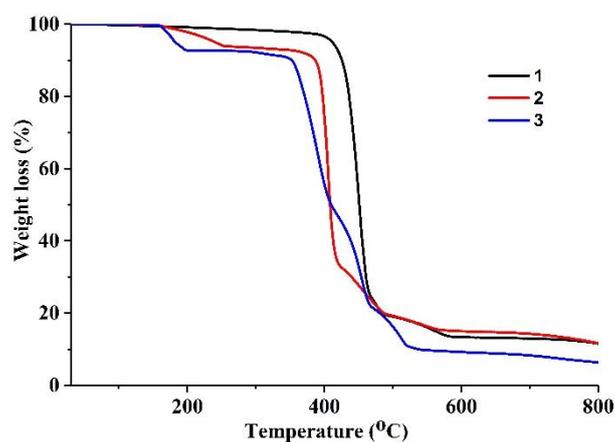
Figure 5. TG curves of **1** – **3**.

Fluorescence properties

According to the previous studies, MOFs based on d^{10} metal ions have been widely investigated as potential fluorescent materials. [33] Therefore, the fluorescence properties of compounds **2** and **3**, as well as the corresponding free ligand dip, were investigated in the solid state at room temperature. As depicted in Figure **5**, dip exhibits an emission band at 398 nm upon excited at 363 nm, while the emission bands of compounds **2** and **3** are observed at 424 and 416 nm under excitation at 374 and 376 nm, respectively. Given that metal ions with d^{10} configurations are difficult to oxidize or reduce, the emissions of **2** and **3** are neither metal-to-ligand charge transfer (MLCT) nor ligand-to-metal charge transfer (LMCT). Therefore, they could be assigned to the intraligand or interligand transitions and the red-shift for the emission bands could be ascribed to the coordination with the Cd(II)/Zn(II) ions. [34]
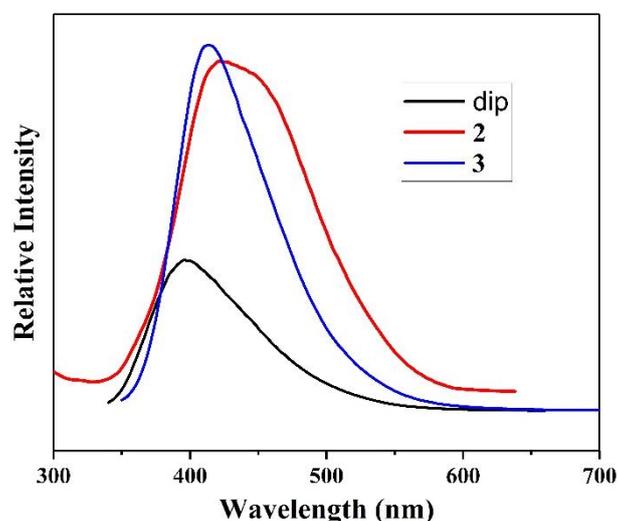
Figure 6. The emission spectra of dip, **2** and **3**.

Conclusion

In summary, we report the synthesis of three new 2D MOFs based on the organic ligand dip with the formula of $[Co(dip)_2(SCN)_2]$ (**1**), $\{[Cd(dip)_2(H_2O)_2]\cdot(NO_3)_2\}$ (**2**) and $\{[Zn(dip)_2(H_2O)_2]\cdot(ClO_4)_2\}$ (**3**). In these three 2D MOFs, all the metal ions exhibit octahedral geometries with four nitrogen atoms from the imidazole units of ligands located in the coordination plane while the anion SCN^- or water molecules bind in the axial direction in the mono-coordinated mode, which thus results in the 2D coordination structure. The final 3D supramolecular frameworks are generated through various non-covalent interactions, such as $\pi\cdots\pi$ and $C-H\cdots\pi$ interactions. The results show that the metal centers with the same coordination geometries can adopt the same structural framework under the same synthetic conditions, even if the counteranions possess different charges, coordination ability and size. Furthermore, the fluorescence properties of **2** and **3** were investigated and exhibited strong emissions.

Acknowledgments

References:

[1] H. Furukawa, K.E. Cordova, M. O'Keeffe, O.M. Yaghi, Science, 341 (2013) 1230444.

[2] N. Stock, S. Biswas, Chem Rev, 112 (2012) 933-969.

[3] P. Li, N.A. Vermeulen, X. Gong, C.D. Malliakas, J.F. Stoddart, J.T. Hupp, O.K. Farha, Angew Chem Int Ed Engl, 55 (2016) 10358-10362.

[4] J.R. Li, R.J. Kuppler, H.C. Zhou, Chem Soc Rev, 38 (2009) 1477-1504.

[5] G. Liu, A. Cadiau, Y. Liu, K. Adil, V. Chernikova, I.D. Carja, Y. Belmabkhout, M. Karunakaran, O. Shekhah, C. Zhang, A.K. Itta, S. Yi, M. Eddaoudi, W.J. Koros, Angew Chem Int Ed Engl, 57 (2018) 14811-14816.

[6] Y.B. Huang, J. Liang, X.S. Wang, R. Cao, Chem Soc Rev, 46 (2017) 126-157.

[7] H. Jia, Y. Yao, J. Zhao, Y. Gao, Z. Luo, P. Du, Journal of Materials Chemistry A, 6 (2018) 1188-1195.

[8] L. Wang, Y. Han, X. Feng, J. Zhou, P. Qi, B. Wang, Coordination Chemistry Reviews, 307 (2016) 361-381.

[9] M.D. Allendorf, C.A. Bauer, R.K. Bhakta, R.J. Houk, Chem Soc Rev, 38 (2009) 1330-1352.

[10] Z. Hu, B.J. Deibert, J. Li, Chem Soc Rev, 43 (2014) 5815-5840.

[11] B. Li, H.M. Wen, Y. Cui, W. Zhou, G. Qian, B. Chen, Adv Mater, 28 (2016) 8819-8860.

[12] A. Dhakshinamoorthy, A.M. Asiri, H. Garcia, Angew Chem Int Ed Engl, 55 (2016) 5414-5445.

[13] Y. Cui, B. Li, H. He, W. Zhou, B. Chen, G. Qian, Acc Chem Res, 49 (2016) 483-493.

[14] S.-L. Li, Q. Xu, Energy & Environmental Science, 6 (2013).

[15] K. S. Novoselov, A. K. Geim, S. V. Morozov, D. Jiang, Y. Zhang, S. V. Dubonos, I. V. Grigorieva, A.A. Firsov, Science, 306 (2004) 666-669.

[16] X. Xiao, H. Wang, P. Urbankowski, Y. Gogotsi, Chem Soc Rev, 47 (2018) 8744-8765.

[17] H. Zhang, M. Chhowalla, Z. Liu, Chem Soc Rev, 47 (2018) 3015-3017.

[18] W. Zhao, J. Peng, W. Wang, S. Liu, Q. Zhao, W. Huang, Coordination Chemistry Reviews, 377 (2018) 44-63.

[19] M. Zhao, Y. Huang, Y. Peng, Z. Huang, Q. Ma, H. Zhang, Chem Soc Rev, 47 (2018) 6267-6295.

[20] M. Xu, S.S. Yang, Z.Y. Gu, Chemistry, 24 (2018) 15131-15142.

[21] H. Nagatomi, N. Yanai, T. Yamada, K. Shiraishi, N. Kimizuka, Chemistry, 24 (2018) 1806-1810.

[22] Y.H. Luo, C. Chen, C. He, Y.Y. Zhu, D.L. Hong, X.T. He, P.J. An, H.S. Wu, B.W. Sun, ACS Appl Mater Interfaces, 10 (2018) 28860-28867.

[23] J. Liu, H. Yu, L. Wang, Z. Deng, K.-u.-R. Naveed, A. Nazir, F. Haq, Inorganica Chimica Acta, 483 (2018) 550-564.

[24] L. Cao, T. Wang, C. Wang, Chinese Journal of Chemistry, 36 (2018) 754-764.

[25] M. Zhao, Q. Lu, Q. Ma, H. Zhang, Small Methods, 1 (2017).

[26] H. Liu, X.-N. Kan, C.-Y. Wu, Q.-Y. Pan, Z.-B. Li, Y.-J. Zhao, Chinese Journal of Polymer Science, 36 (2017) 425-444.

[27] J. Park, A.C. Hinckley, Z. Huang, D. Feng, A.A. Yakovenko, M. Lee, S. Chen, X. Zou, Z. Bao, J Am Chem Soc, 140 (2018) 14533-14537.

[28] R. Makiura, S. Motoyama, Y. Umemura, H. Yamanaka, O. Sakata, H. Kitagawa, Nat Mater, 9 (2010) 565-571.

[29] L. Luo, Y. Zhao, Y. Lu, T.-a. Okamura, W.-Y. Sun, Polyhedron, 38 (2012) 88-96.

[30] SAINT, *Program for Data Extraction and Reduction*, Bruker AXS, Inc., Madison, WI, 2001.

[31] G. M. Sheldrick, *SADABS*, *Program for Empirical Adsorption Correction of Area Detector Data*. University of Gottingen, Gottingen, Germany, 2003.

[32] (a) G. M. Sheldrick, *SHELXS-97, Program for the Crystal Structure Solution*, University of Gottingen, Gottingen, Germany, 1997; (b) G. M. Sheldrick, *SHELXL-97, Program for the Crystal*

Structure Solution, University of Gottingen, Gottingen, Germany, 1997.